*Hyperfine Interactions* **132:** 75–103, 2001.
© 2001 *Kluwer Academic Publishers. Printed in the Netherlands.*


# Effects of QED and Beyond from the Atomic Binding Energy ⋆

G. SOFF[1], I. BEDNYAKOV[1,2], T. BEIER[3], F. ERLER[1], I. A. GOIDENKO[2], U. D. JENTSCHURA[1,4], L. N. LABZOWSKY[2], A. V. NEFIODOV[5], G. PLUNIEN[1], R. SCHÜTZHOLD[1] and S. ZSCHOCKE[1]

[1] *Technische Universität Dresden, Mommsenstr. 13, D-01062 Dresden, Germany*
[2] *St. Petersburg State University, 198904 St. Petersburg, Russia*
[3] *Gesellschaft für Schwerionenforschung, Planckstr. 1, D-64291 Darmstadt, Germany*
[4] *Laboratoire Kastler–Brossel, Case 74, 4 Place Jussieu, F-75252 Paris Cedex 05, France*
[5] *Petersburg Nuclear Physics Institute, 188350 Gatchina, St. Petersburg, Russia*

**Abstract.** Atomic binding energies are calculated at utmost precision. A report on the current status of Lamb-shift predictions for hydrogenlike ions, including all quantum electrodynamical corrections to first and second order in the fine structure constant $\alpha$ is presented. All relevant nuclear effects are taken into account. High-precision calculations for the Lamb shift in hydrogen are presented. The hyperfine structure splitting and the $g$ factor of a bound electron in the strong electromagnetic field of a heavy nucleus is considered. Special emphasis is also put on parity violation effects in atomic systems. For all systems possible investigations beyond precision tests of quantum electrodynamics are considered.

**Key words:** atomic binding energy, electron $g$-factor, highly-charged ions, Lamb shift, parity violation, quantum electrodynamics.

## 1. Introduction

Quantum Electrodynamics (QED) can claim to be one of the most precisely tested theories of physics. One impressive example is the $g$ factor of the free electron which is known today as

$$g_{\text{free}} = 2 + 2 \times 1\,159\,652\,188.4(4.3) \times 10^{-12} \qquad \text{(Experiment [1])}$$
$$g_{\text{free}} = 2 + 2 \times 1\,159\,652\,216.0(1.2)(67.8) \times 10^{-12} \qquad \text{(Theory [2])}.$$

(The second error indicated in the second line is due to the value of $\alpha$ employed in this calculation [3].) Similar precisions are nowadays obtained in systems like positronium or the Lamb shift in hydrogen where insufficiently known nuclear parameters limit the accuracy of theoretical predictions [4, 5]. The electric field involved in all these systems is rather low, however, compared to the strongest electromagnetic fields accesible to experimental investigation today. In atomic systems, these strong fields are obtained by stripping all but one electron from a heavy atom,

⋆ Dedicated to Prof. A. Wapstra on the occasion of his 78th birthday.

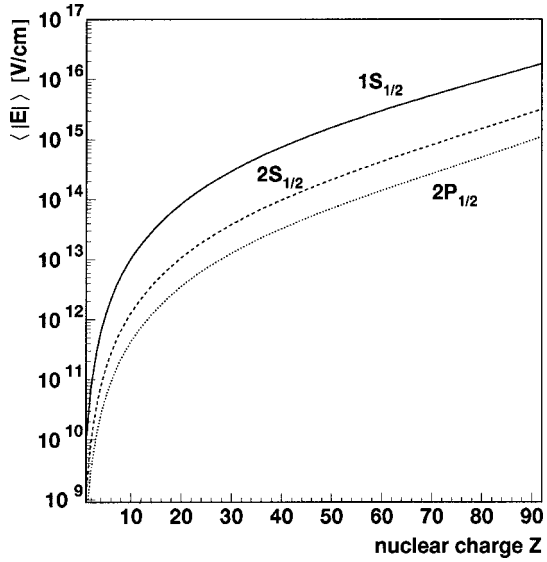


*Figure 1.* Expectation value of the electric field strength for the lowest-lying states of a hydrogenlike atom in the range $Z = 1$–92.

e.g., lead or uranium. The single electron is bound in a system similar to hydrogen, and the whole system is therefore called hydrogen-like system. The expectation value of the electric field strength in these systems is depicted in Figure 1. The field strength at the nuclear surface is even higher. For example, at the surface of a uranium nucleus, $|\mathbf{E}| \cong 2 \cdot 10^{19}$ V/cm. This is only a factor of 2 less than the field strength in superheavy systems with $Z \geqslant 170$ where spontaneous pair production is predicted to take place if the total charge can be confined in a sufficiently small volume for a sufficiently long time [6–8]. It seems evident that in such strong fields 'normal' atomic physics – valid for a hydrogen atom where the field probed by the electron is six orders of magnitudes smaller – may be questioned. A precise knowledge about the validity of QED in strong external fields is also very promising for the detection of new physics beyond QED [9]. Thus it is a primary goal to explore the behaviour of electrons in some of the strongest electromagnetic fields accessible to experimental investigation. Additional evidence can be obtained from muonic atoms because the muon is localized much closer to the nucleus and probes therefore even stronger fields. On the other hand, it is also more sensitive to nuclear effects that are theoretically less well known.

In atoms, the coupling of the electron with the binding field of the nucleus is determined by the coupling constant $Z\alpha$ where $Z$ is the nuclear charge number and $\alpha \approx 1/137$ is the fine structure constant. In highly charged ions like uranium, the coupling constant is no longer a small parameter but amounts to $Z\alpha \approx 0.6$ and therefore a perturbation expansion in $Z\alpha$ becomes meaningless. In contrast, most approaches for the calculation of QED effects in low-$Z$ atoms like hydrogen still

employ such an expansion. In heavy ions, the interaction with the Coulomb field of the nucleus has to be considered to all orders in $Z\alpha$. Bound-state QED provides the relativistic description of an electron in highly charged atomic systems. To test the predictions of this theory with utmost precision is a major challange in todays atomic physics. This review is focused on the recent developments in this exciting area. The examples given here will indicate the predictive power of QED in 'simple systems' where many-body effects do not have to be considered except for nuclear structure calculations. The paper is organized as follows:

In Section 2 we will consider the present status in the evaluation of all QED corrections to the Lamb shift in hydrogen-like uranium and lead and compare theoretical and experimental results. The general theoretical and experimental precision of Lamb shift measurements will be discussed, and an interesting future direction of research will be mentioned. In Section 3 the hyperfine splitting of atomic levels is considered. We will report on the present status of the hyperfine splitting effect in hydrogen- and lithiumlike ions and we will compare the theoretical results with the available experimental values. Another quantity accessible for high-precision experiments is the $g$ factor of a bound electron which is also in the scope of Section 3.

In Section 4 parity violating effets in atomic systems will be considered. The advantages of investigating these effects in highly charged ions will be underlined and a new experiment for detecting a parity violation in heliumlike europium and gadolinium is proposed.

## 2. Lamb-shift calculations

The term *Lamb shift* refers to the difference between the Dirac energy eigenvalue of a single atomic level and its actual value which is shifted due to nuclear and QED effects. The binding energy of an atomic level is one of the quantities best to measure and therefore QED effects are well detectable. Precise measurements in hydrogenlike heavy ions nowadays concentrate on uranium [10] where the best measurement recently was achieved by Stöhlker *et al.* [11, 12]. Also in gold [13], lead [14], and bismuth [15] the ground state Lamb shifts were investigated.

The major contributions to the $1s_{1/2}$ Lamb shift are the radiative corrections of order $\alpha$ (Figure 2), and also the effect of the nuclear size which accounts for the

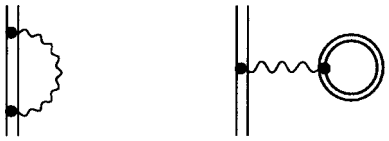


*Figure 2.* The QED corrections of order $\alpha$, self energy (SE) and vacuum polarization (VP). The double solid line denotes the bound electron and the wavy line indicates the photon.

finite extension of the nuclear charge distribution. Therefore the potential that is present in the Dirac equation changes and the wave functions and energy eigenvalues are slightly altered. Examples can be found, e.g., in [16]. For uranium, even the different models for the shape of the nucleus at a fixed size ($\langle r^2 \rangle^{1/2} = 5.860 \pm 0.002$ fm) cause differences in the K-shell binding energy of nearly one eV.

The two major QED corrections are self energy and vacuum polarization. The self energy (SE) is the result of the emission and reabsorption of a photon by an electron. For high-$Z$ ions, it has been calculated employing many different methods, beginning from the pioneering elaborations of Brown *et al.* [17] and Desiderio and Johnson [18] to the more accurate approach developed by Mohr [19, 20]. Blundell and Snyderman presented an alternative approach [21, 22] of calculating the first-order self energy also in a non-Coulomb potential.

The first-order vacuum polarization (VP) correction accounts for the interaction of the electron with a virtual electron-positron pair in the field of the nucleus. It is commonly divided into two major parts, the charge divergent but nowadays well-known Uehling part [23–26] and the finite Wichmann–Kroll part [27] which was evaluated by Gyulassi [28] and later with high precision by Soff and Mohr [29], and by another approach also by Fainshtein *et al.* [30]. Persson *et al.* could even improve the numerical accuracy [31].

The finite nuclear size has also an effect on the radiative corrections. For uranium, the difference between the self-energy correction with and without considering the nuclear size amounts to more than 1% [32] and therefore the influence of the nuclear size on the radiative corrections should be taken into consideration at least for heavy systems with $Z > 50$. An elaborated investigation on this topic for both self energy and vacuum polarization is given in [33]. The results of all these contributions for hydrogen-like uranium and lead are depicted in Table I, together with the contributions of order $\alpha^2$ and the recoil contributions.

All present experimental results can be theoretically well explained by considering the effect of the finite nuclear size and the QED corrections of order $\alpha$ as discussed above. However, at the GSI in Darmstadt, a precision of about 1 eV in measurements of the ground-state Lamb shift seems likely in the near future [12]. At this level, QED corrections of order $\alpha^2$ have to be taken into account. The complete set of radiative corrections is displayed in Figures 3(a)–(k). These diagrams are naturally divided into separately gauge invariant subsets: SESE (a), (b), (c); VPVP (d); VPVP (e), (f); SEVP (g), (h), (i); and S(VP)E (k). In addition to a complicated renormalization scheme, the calculation of higher-order QED corrections also requires the application of special numerical methods to perform multiple summations over the complete eigenfunction spectrum of the Dirac equation for a bound electron. Only recently this task was completed for the last missing contributions, the so-called reducible part of the SESE (a) diagram together with the SESE (b) and (c) diagrams. Now all of these corrections have been numerically calculated for the ground state of hydrogenlike uranium and lead [34]. The so-called irreducible contribution SESE (a) can be separately renormalized and

*Table I.* Lamb-shift contribution for the ground state of $^{238}U^{91+}$ and $^{208}Pb^{81+}$ (in eV), including the full recoil contribution. The finite nuclear-size correction for uranium is calculated for a Fermi distribution with $\langle r^2\rangle^{1/2} = 5.860 \pm 0.002$ fm. The finite nuclear-size correction for lead is calculated for a Fermi distribution with $\langle r^2\rangle^{1/2} = 5.505 \pm 0.001$ fm. Known error-margins are linearly added

| Corrections (in eV): | $^{238}U^{91+}$ | | $^{208}Pb^{81+}$ | |
|---|---|---|---|---|
| Finite nuclear size | 198.82 | ±0.10 | 67.25 | ±0.02 |
| Self energy (order $\alpha$) | 355.05 | | 226.33 | |
| Vacuum polarization (order $\alpha$) | −88.60 | | −48.41 | |
| SESE (a) (irred.) | −0.97 | | −0.51 | |
| SESE (a) (red.) (b), (c) | 1.28 | ±0.15 | 0.73 | ±0.09 |
| VPVP (d) | −0.22 | | −0.09 | |
| VPVP (e) | −0.15 | | −0.07 | |
| VPVP (f) (Uehling approx.) | −0.60 | ±0.10 | −0.34 | |
| SEVP (g), (h), (i) | 1.12 | | 0.53 | |
| S(VP)E (k) (Uehling approx.) | 0.13 | | 0.07 | |
| Total recoil | 0.46 | | 0.37 | |
| Nuclear polarization | −0.20 | ±0.10 | 0.00 | |
| Lamb shift (theory) | 466.12 | ±0.45 | 245.86 | ±0.11 |
| Lamb shift (experiment) | 469. | ±16 | 290. | ±75 |

evaluated. It denotes that part of the SESE (a) diagram where the energy of the intermediate electron states between the two self-energy loops is different from the energy of the state under consideration. This contribution has been first calculated by Mitrushenkov *et al.* [35] for the nuclear charge numbers $Z = 70$, 80, 90, and 92, and recently for arbitrary values of $Z$ in [36, 37]. Although the obtained results are in fair agreement for high $Z$, a discrepancy between these in [36] and [37] has been observed for the case of low and intermediate $Z$ values. Only the results of [37] agree with an analytical expansion based on powers and logarithms of $Z\alpha$ [38]. The reason for this discrepancy is under current investigation and two recent works devoted to this subject again end up with different conclusions: the calculation of Yerokhin [39] supports [36] whereas Manohar and Stewart [40] find the same logarithmic term as Karshenboim in [38]. It would be not the first time however, that modern high-$Z$ methods prove to be more successful also for low $Z$ than the conventional $Z\alpha$ expansion [41]. For the high-$Z$ region, there is no doubt about the results presented in Table I.

The VPVP contributions (e) and (f) (also known as Källén–Sabry corrections) have been investigated in Uehling approximation [42, 43]. Calculating the dominant Uehling part of the lowest order VP correction results in a precision of about

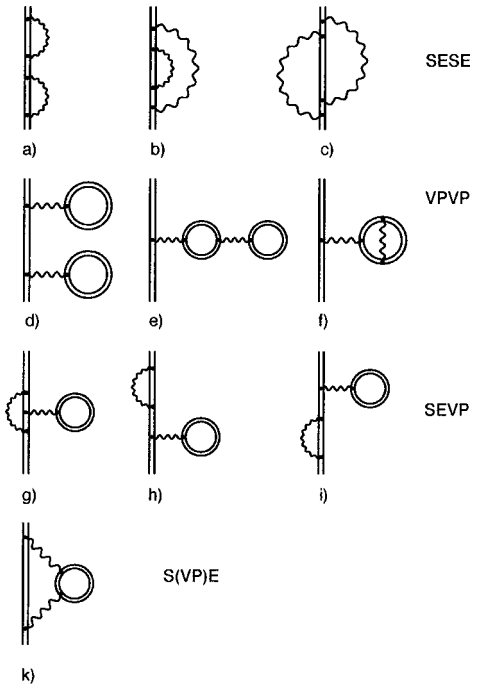


*Figure 3.* Feynman diagrams corresponding to the radiative corrections of order $\alpha^2$ in hydrogenlike ions.

5% for the ground state of hydrogenlike uranium and lead ions. In the Uehling approximation one restricts to the first term in a $Z\alpha$ expansion of the bound electron propagator in the electron loop. This also corresponds to the expansion of the bound propagator in terms of the nuclear potential. Recently the VPVP (e) contribution has been determined to all orders in $Z\alpha$ [44]. In this case the inaccuracy of the Uehling approximation turned out to be about 25%. The VPVP (d) contribution was considered in [31] and tabulated in [45]. The SEVP (g), (h), and (i) contributions were evaluated in [46] employing the Uehling approximation and in the exact form in [47]. The inaccuracy of Uehling approximation for hydrogenlike uranium amounts to only 2% in this case. The S(VP)E (k) contribution has been calculated only in Uehling approximation up to now [47, 48]. A recent overview about all first- and second-order QED corrections is presented in [49].

In addition to the QED corrections of order $\alpha^2$, the internal structure ('polarizability') of the nucleus and the nuclear recoil effect cause additional binding-energy corrections of the same order of magnitude as these QED corrections. The nuclear-polarization contribution was derived and evaluated in the framework of an effective photon propagator in [50–52]. The recoil effect accounts for a non-infinitely heavy nucleus and takes into account its movement. Nonrelativistically this can be considered by the reduced mass of the electron, an approximation which is more than 50% wrong for heavy hydrogenlike systems like uranium. The com-

plete effect to all orders in $Z\alpha$ was calculated in [53, 54] for point-like nuclei and in [55] for extended nuclei. The extension of the nuclear charge distribution reduces the effect by about 10% in the case of $U^{91+}$. In Table I the results are compiled for uranium and lead together with all QED corrections of order $\alpha$ and $\alpha^2$ and also with the nuclear effects. We point out that the compilation in this table does not follow the convention of [56] who do not include the nonrelativistic reduced-mass correction in the Lamb shift because it does not contribute to the 'classical' $2s_{1/2}$–$2p_{1/2}$ splitting in low-$Z$ atoms. For high-$Z$ systems, however, a complete recoil correction inherently includes the nonrelativistic reduced-mass correction and there is no sense to consider this contribution separately [57]. All our present results allow for high-precision tests of QED in the strong field of the nucleus that are expected to be experimentally available in the near future.

The high-precision calculations for high-$Z$ systems also influence the predictive power in the low-$Z$ region where higher precision is gained by including more and more terms of an expansion in the interaction with the binding field, i.e., in powers of $Z\alpha$ and some logarithmic terms. For an overview about these 'analytical' techniques, we refer to [58]. The precise determination of radiative corrections by numerical calculations even for low nuclear charge numbers $Z$ is currently an emerging field [59]. Here, we will focus on the one-photon self energy, which constitutes the dominant contribution to the Lamb shift in hydrogen by two orders of magnitude.

One of the calculational challenges in the regime of low nuclear charge are numerical cancellations. In order to understand the origin of the numerical cancellations it is necessary to consider the renormalization of the self energy. The renormalization procedure postulates that the self energy is essentially the effect on the bound electron due to the self interaction with its own radiation field, minus the same effect on a free electron. There it is absorbed in the mass of the electron and therefore not observable. The self energy of the bound electron is the difference of two large quantities. Terms associated with renormalization counterterms are of order unity in the $Z\alpha$-expansion, whereas the residual effect is of order $(Z\alpha)^4$. This corresponds to a loss of only one significant figure at $Z = 92$, but roughly 9 significant digits at $Z = 1$. Accurate numerical methods have to be employed, and the convergence of certain angular momentum expansions has to be accelerated by powerful numerical algorithms (see, e.g., [60]) which reduce the computation time by roughly three orders of magnitude.

We start our discussion here from the well-known (regularized and renormalized) expression for the one-photon self energy $\Delta E_{\mathrm{SE}}$,

$$\Delta E_{\mathrm{SE}} = \lim_{\Lambda\to\infty}\left\{-\mathrm{i}\,e^2\,\mathrm{Re}\int_{\mathcal{C}}\frac{\mathrm{d}\omega}{2\pi}\int\frac{\mathrm{d}^3\mathbf{k}}{(2\pi)^3}\,D_{\mu\nu}\big(k^2,\Lambda\big)\right.$$
$$\left.\times\langle\psi|\alpha^\mu\exp(\mathrm{i}\mathbf{k}\cdot\mathbf{x})G(E_{\mathrm{n}}-\omega)\alpha^\nu\exp(-\mathrm{i}\mathbf{k}\cdot\mathbf{x})\,|\psi\rangle-\Delta m\right\}, \quad (1)$$

where $G$ denotes the Dirac–Coulomb propagator,

$$G(z) = \frac{1}{\boldsymbol{\alpha} \cdot \mathbf{p} + \beta + V - z}, \tag{2}$$

and $\Delta m$ is the cutoff-dependent one-loop mass-counter term,

$$\Delta m = \frac{\alpha}{\pi} \left( \frac{3}{4} \ln \Lambda^2 + \frac{3}{8} \right) \langle \beta \rangle. \tag{3}$$

Here, $\Lambda$ serves as a cutoff parameter. The photon propagator $D_{\mu\nu}(k^2, \Lambda)$ in Equation (1) is given by (in Feynman gauge)

$$D_{\mu\nu}(k^2, \Lambda) = -\left( \frac{g_{\mu\nu}}{k^2 + \mathrm{i}\epsilon} - \frac{g_{\mu\nu}}{k^2 - \Lambda^2 + \mathrm{i}\epsilon} \right). \tag{4}$$

The contour $\mathcal{C}$ used in the numerical calculation is *not* the Feynman contour but represents the mathematically equivalent contour depicted in Figure 4. The analytic structure of the propagators plays an important role in the evaluation, and the choice of the contour has to reflect this structure which is indicated by the branch cuts in Figure 4, while at the same time providing a convenient basis for the numerical evaluations (as discussed below). The energy variable $z$ in Equation (2) assumes the value

$$z = E_{\mathrm{n}} - \omega, \tag{5}$$

where $E_{\mathrm{n}}$ is the Dirac energy of the atomic state, and $\omega$ denotes the complex-valued energy of the virtual photon. It is understood that the limit $\Lambda \to \infty$ is taken *after* all integrals in Equation (1) are evaluated.

The contour $\mathcal{C}$ naturally leads to a separation of the two scales in the self-energy problem: the atomic energy scale $(Z\alpha)^2 m$ and the relativistic electron mass

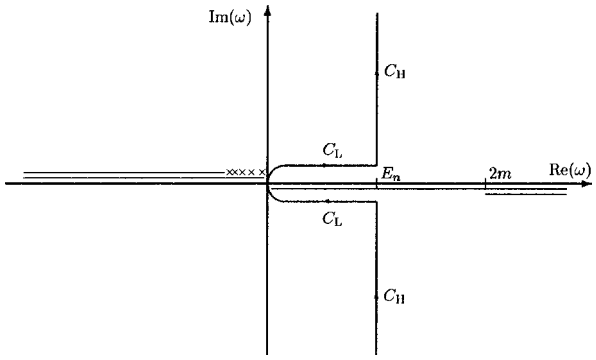


*Figure 4.* Integration contour $\mathcal{C}$ for the integration over the energy $\omega = E_{\mathrm{n}} - z$ of the virtual photon. The contour $\mathcal{C}$ consists of the low-energy contour $C_{\mathrm{L}}$ and the high-energy contour $C_{\mathrm{H}}$. Lines shown displaced directly below and above the real axis denote branch cuts from the photon and electron propagator. Crosses denote poles originating from the discrete spectrum of the electron propagator.

scale. It is perhaps interesting to note that similar contours are also employed in analytic evaluations of the self energy [41, 61, 62], which are based on the $Z\alpha$-expansion (there, too, a separation of the two energy scales is necessary). The decisive observation is that the separation of the scales by an appropriate choice of the contour facilitates the numerical evaluations considerably. Different techniques are employed for the high- and the low-energy part.

In the low-energy part, the most challenging problem is the accurate numerical evaluation of the bound electron propagator to the required relative precision of $10^{-24}$, whereas the convergence of the partial wave expansion represents a less involved problem. Resummation techniques [63] which associate a finite value to an otherwise divergent series are used in this part of the calculation. Observe that the crosses in Figure 4 are shifted infinitesimally above the positive real axis for excited states; the corresponding imaginary contributions to the integral (1) yield the autoionization decay width. For the energy shift, we are only interested in the real part of the radiative correction. For excited states, the subtraction of the pole contributions of low-lying states to the required accuracy represents another challenge in numerical calculations (this subtraction necessarily has to be done before the final photon-energy integrations are carried out). Difficulties associated with the regime of ultra-soft photons and the subtraction of the pole contributions necessitate a further separation of the low-energy part into an infrared part and a middle-energy contribution (see Figure 5).

We now discuss one of the fundamental differences between numerical and analytic evaluations. The free electron propagator

$$F = \frac{1}{\boldsymbol{\alpha} \cdot \mathbf{p} + \beta - z} \tag{6}$$

and the full electron propagator $G$ defined in Equation (2) fulfill the following exact identity,

$$G = F - F\,V\,F + F\,V\,G\,V\,F.$$

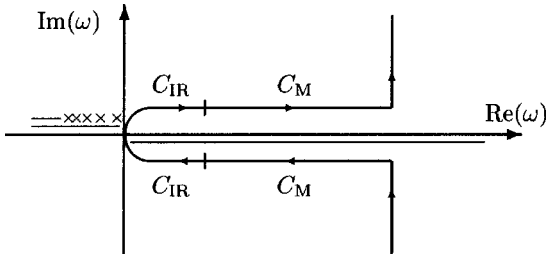


*Figure 5.* Separation of the low-energy contour $C_{\mathrm{L}}$ into the infrared part $C_{\mathrm{IR}}$ and the middle-energy part $C_{\mathrm{M}}$. As in Figure 4, the lines directly above and below the real axis denote branch cuts from the photon and electron propagator. At the separation, we have $\mathrm{Re}\,\omega = 0.1\,E_{\mathrm{n}}$.

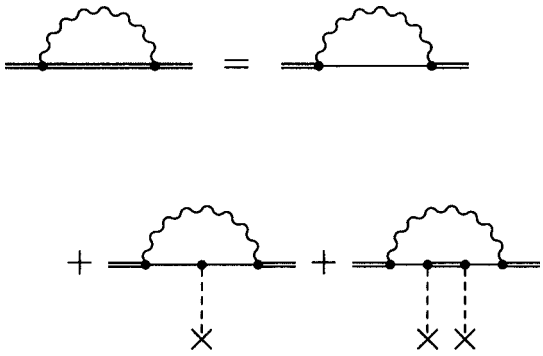

*Figure 6.* The exact expansion of the bound electron propagator in powers of the binding field leads to a zero-potential, a one-potential, and a many-potential term. The dashed lines denote Coulomb photons, the crosses denote the interaction with the (external) binding field.

This exact identity is used in numerical calculations (a diagrammatic representation is shown in Figure 6). The identity leads naturally to a separation of the one-photon self energy into a zero-vertex, a single-vertex, and a many-vertex term (also represented diagrammatically in Figure 6). In analytic calculations, advantage is taken of the iterated form of this identity,

$$G = F - F\,V\,F + F\,V\,F\,V\,F - \cdots .$$

This analytic expansion in $V \cong Z\alpha$ necessarily has to be terminated at a finite order; the error made in the termination of the expansion at order $(Z\alpha)^6$ in comparison to the nonperturbative result is 28 kHz for atomic hydrogen. This has to be compared to an experimental accuracy of currently 46 Hz for the $1s_{1/2}$–$2s_{1/2}$ transition. The nonperturbative numerical calculation overcomes the accuracy limit set by the termination of the $Z\alpha$-expansion and leads to predictions which match the current experimental precision.

Slow convergence of the $Z\alpha$-expansion and the exceeding number of analytic terms in higher order are likely to represent considerable problems for the conceivable further improvement of analytic evaluations. At the same time, the nonperturbative numerical evaluations provide a consistency check of the extensive work on analytic calculations. As of today, full consistency between the analytic and numerical approaches to the Lamb-shift problem is observed [59]. For the numerical values of the corrections for hydrogen (K and L shell) at the 1 Hz precision level we refer to our separate article in this volume [64].

This very high theoretical precision is matched by a corresponding one on the experimental side. Absolute frequency measurements have become possible in part due to optical frequency divider chains and frequency combs. These bridge the frequency gaps between frequency standards and the transition frequencies in the optical and ultraviolet range. Currently, the most precisely determined transition is the $1s_{1/2}$–$2s_{1/2}$ transition in hydrogen which was measured to be 2 466 061 413 187 103 (46) Hz, i.e., to a precision of $1.8 \times 10^{-14}$ [65]. From two different transitions

in hydrogen, it is possible to derive both the $1s_{1/2}$ Lamb shift and also the Rydberg constant $R_\infty = \alpha^2 c m_e/(2h)$. Its value is given at present to be $R_\infty = 10\,973\,731.568\,549(83)\,\mathrm{m}^{-1}$ [66]. Aiming for an even higher accuracy, measurements would be able to detect a time variation in the fine structure constant $\alpha$. Absolute frequency measurements can be reproduced years later whereas measurements that monitor only relative shifts in $\alpha$ need to be in continuous operation. The current limit on variation of $\alpha$ with time is given by comparing a hydrogen maser with a Hg microwave atomic clock over a range of 140 days [67],

$$\left|\frac{\dot{\alpha}}{\alpha}\right| < 3.7 \times 10^{-14}\,\mathrm{yr}^{-1}. \tag{7}$$

This number refers to a time variation in the recent epoch. Looking on longer time scales or on astrophysical data, the boundary becomes even more stringent but for earlier epochs of the universe [68]. Indications for an *existing* variation of $\alpha$ with time are taken from observations of spectra of very far red-shifted quasars [69] where the data might indicate a small *negative* $\dot{\alpha}$ (i.e., $\alpha$ seemed to have been *larger* in former times) and no other explanation has been found yet. The data are too poor to give clear evidence, however.

It is beyond the scope of the present article to discuss the underlying theory for the time variation of fundamental constants in detail. We are just going to point to some major articles in this field. The possible non-constancy of fundamental constants was already considered by Dirac [70]. Nowadays, the time variation of $\alpha$ is predicted by a number of theories such a string theory (e.g., [71–73]). In superstring theories, Einstein's equations of General Relativity are obtained in a straightforward manner but with a scalar extension. This scalar particle links the time variation of $\alpha$ to the Hubble constant, $\dot{\alpha} \sim H_0$ [73]. Alternatively, theories have been considered which introduce new scalar fields [74]. Their coupling to the Maxwell scalar $F_{\mu\nu}F^{\mu\nu}$ allows for a time variation of $\alpha$. The fine structure constant is not the only 'constant' which might show a possible variation in time. In Kaluza–Klein theories, the unification of forces takes place in an enlarged space-time of $4 + N$ dimensions where $N$ is the number of additional spatial dimensions and $N \geqslant 7$. These extra dimensions are supposed to form a very small compact manifold with a mean radius $R_{\mathrm{KK}}$ where $R_{\mathrm{KK}}$ is thought to be of the order of the Planck length $l_{\mathrm{P}} = \sqrt{(\hbar G_N)/c^3} \simeq 1.6 \times 10^{-35}$ m. Here $G_N$ denotes the gravitational constant. In Kaluza–Klein theories, an expanding universe leads quite naturally to $\dot{R}_{\mathrm{KK}} \neq 0$ [71], and if one allows for a varying $\alpha$ one finds $\dot{\alpha} \sim \dot{G}_N$. In addition, other observables might also change with time such as the masses of non-fundamental particles, e.g., $\mathrm{d}/\mathrm{d}t\,(m_e/m_p) \neq 0$. Godone *et al.* [75] put a limit on the product of the proton's $g$ factor and that mass ratio, $|\mathrm{d}/\mathrm{d}t \ln[g_p\,(m_e/m_p)]| \leqslant 5.4 \times 10^{-13}\,\mathrm{yr}^{-1}$.

From this discussion it is obvious that high-precision experiments together with the widely developed theory of QED are well able to support physicists in their search for new and exciting phenomena beyond the standard model.

## 3. Magnetic effects: Hyperfine structure splitting and *g* factor

Highly charged ions do not only provide a strong electric but also a strong magnetic field. In Figure 7 the expectation value for the magnetic field strength is given for hydrogenlike ions over the whole range of $Z$. It amounts from about $10^{-1}$ T from hydrogen to several times $10^5$ T for the heaviest hydrogenlike ions accessible for experiments. Still, even this enormous field strength leads to only a small influence on the atomic energy levels. As a result of the interaction of an electron in an open shell with this magnetic field, the level splits into sublevels corresponding to the possible values of the total momentum $\mathbf{F} = \mathbf{J} + \mathbf{I}$ of the atom, where $\mathbf{J}$ is the electronic angular momentum and $\mathbf{I}$ denotes the nuclear angular momentum. Only the total angular momentum $\mathbf{F}$ is an observable. For the ground state of hydrogen- and lithiumlike atoms with only one electron in the $1s_{1/2}$ or $2s_{1/2}$ state ($J = 1/2$), this results in a splitting into two sublevels. This level splitting is termed hyperfine structure splitting, and its value can be determined quite accurately by spectroscopic means. The hyperfine structure splitting of the ground state in hydrogen is

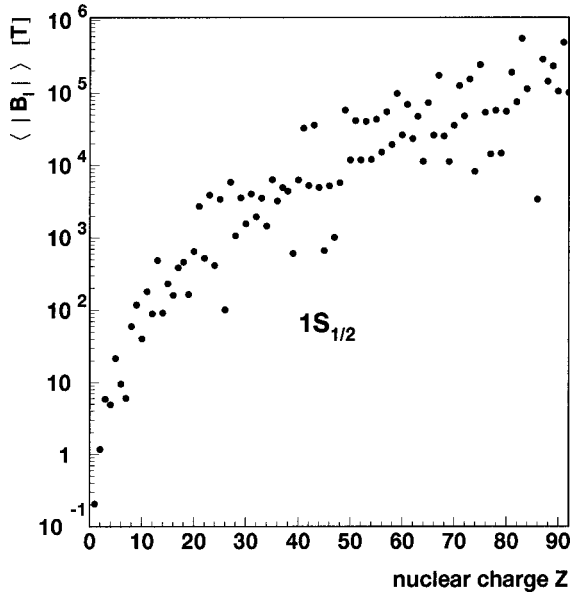


*Figure 7.* Expectation value of the magnetic field strength for the $1s_{1/2}$ state of a hydrogenlike atom in the range $Z = 1$–92. For each $Z$, the odd isotope with the highest natural abundance or longest lifetime was chosen. The nuclear magnetic moments are different for each system and do not follow a simple functional law. Therefore no continuous curve is obtained. The values were calculated employing wave functions for extended nuclear charge distributions.

one of the quantities in nature that is most precisely known but it also demonstrates the theoretical difficulties connected to it. Measurement and theoretical calculation are conventionally not even presented in a comparable way because of effects resulting from the proton structure [56, 76]. They lead to a small deviation from the idealized point-dipole magnetic field, and this deviation still cannot be described in a proper theoretical manner because its exact form is unknown.

The present numbers are

$$\nu_{\mathrm{HFS}} = 1420.405\,751\,766\,7(9)\ \mathrm{MHz} \qquad \text{(Experiment [77, 78])},$$
$$\nu_{\mathrm{HFS}} = 1420.451\,99(10)\ \mathrm{MHZ} + \text{nuclear structure effects} \qquad \text{(Theory [56])},$$

where the nuclear strucure effects include all contributions from the proton, from finite size and mass to form factors and internal structure. Most of the discrepancy between both numbers is already removed if the finite size of the proton is taken into account [79] but the theoretical precision does not increase. In the theoretical value, quantum elctrodynamical effects are included up to the reasonable accuracy.

The theoretical handling of quantum electrodynamical corrections to the hyperfine structure splitting is the same as for the $g$ factor since in both cases radiative corrections to a magnetic perturbation are considered. Up to now, highly charged ions were experimentally investigated aiming for the hyperfine strucutre splitting, at GSI [80–82] as well as at the Lawrence Livermore National Laboratory (USA) [83, 84]. Corresponding to the rather high experimental precision, also theoretical investigations were carried out in particular on the QED contributions of order $\alpha$ to the hyperfine structure splitting in heavy highly charged ions. Again, a perturbation expansion in $Z\alpha$ is not feasible, and the employed computational methods are very similar to those for the Lamb shift.

The ground-state hyperfine structure splitting of hydrogen-like ions can be written in the form

$$\triangle E = \frac{4}{3}\alpha(\alpha Z)^3 \frac{\mu}{\mu_{\mathrm{N}}} \frac{m}{m_{\mathrm{p}}} \frac{2I+1}{2I} mc^2 \big[A(\alpha Z)(1-\delta)(1-\epsilon) + \chi_{\mathrm{QED}}\big], \tag{8}$$

where $m$ is the electron mass, $m_{\mathrm{p}}$ is the proton mass, $\mu$ is the nuclear magnetic moment and $\mu_{\mathrm{N}} = (e\hbar)/(2m_{\mathrm{p}}) \approx 3.152 \times 10^{-8}$ eV/T is the nuclear magneton. The terms in the square brackets represent the four corrections to the classical nonrelativistic hyperfine splitting, i.e., the relativistic factor which for the $1s_{1/2}$ state is given by [85]

$$A(\alpha Z) = \frac{1}{\gamma(2\gamma - 1)} \quad \text{with } \gamma = \sqrt{1-(\alpha Z)^2}, \tag{9}$$

the finite-size nuclear-charge distribution correction $\delta$, the finite-size nuclear-magnetization distribution correction $\epsilon$, and the QED corrections denoted by $\chi_{\mathrm{QED}}$.

The nuclear charge distribution can easily be taken into account, similar to the Lamb-shift case. The wave functions for the electron are calculated by solving

the Dirac equation where the Coulomb potential is slightly modified around the origin. These wave functions are then employed for the hyperfine structure splitting calculations. The uncertainty of this effect is governed by the insufficiently known nuclear charge distribution and does not play any role at the current level of precision for the theoretical predictions of the hyperfine structure splitting. A reasonable nuclear charge distribution, e.g., a two-parameter Fermi distribution, allows to evaluate the effect very easily (e.g, [86]).

The effect due to a deviation from the point-dipole model for the nuclear magnetization distribution is often termed Bohr–Weisskopf effect, after Å. Bohr and V. Weisskopf who performed the first numerical investigations [87, 88]. They employed a so-called single-particle model where the extended magnetization distribution is due to a single valence nucleon moving around a core formed by all other nucleons. One elaborated form of this model was employed to obtain numerical values for that effect in the range $Z = 49$–$83$ for hydrogen- and lithiumlike ions [86, 89, 90]. For $^{209}Bi^{82+}$ a related model with the valence proton moving relativistically was also considered [91, 92]. It gives similar results. A number of other approaches also try to model the magnetization distribution of the nucleus due to some outer valence nucleon [93] or treat the whole magnetization distribution on a purely phenomenological base by introducing parameters that allow to model nearly any distribution of the magnetization within the nucleus [94]. The total interaction of all nucleons, however, is not taken into account in any of these models. An approach pointing more into that direction is the so-called 'dynamical-correlation model' first evaluated by Arima and Horie [95, 96] and applied to highly charged ions by Tomaselli *et al.* [97, 98]. This model, however, depends even more than those mentioned before on input parameters that have to be obtained from independent experiments. Therefore it is highly sensitive to uncertainties from nuclear physics. An elaborated discussion on the current difficulties estimating the Bohr–Weisskopf effect is given in a recent review [99].

The QED corrections of order $\alpha$ to a bound electron interacting with a perturbing magnetic field are given in Figure 8. They have all been calculated during the last decade by several independent groups for the $1s_{1/2}$ and the $2s_{1/2}$ state [86, 90, 100–105] and their values are well established. Unfortunately, their magnitude is of similar size as the uncertainty of the Bohr–Weisskopf effect caused by the model-like structure which has to be employed for the nuclear magnetization distribution. Therefore any precision test of bound-state QED by measuring the hyperfine structure splitting in any highly charged ion is prevented until a reliable model for the nuclear structure becomes available.

It is possible, however, to combine measurements of the hyperfine structure splitting in hydrogenlike and lithiumlike ions of the same species, as was pointed out by Shabaev [106, 107]. By extracting a value for the Bohr–Weisskopf effect from one experiment, its magnitude for the other charge state of the ion can be adjusted and its uncertainty is much less than that due to employing different

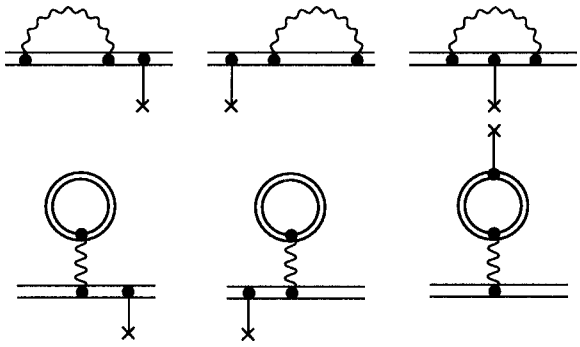

*Figure 8.* The self-energy and vacuum-polarization correction to a bound electron perturbed by an external magnetic field. The solid line terminated by a cross denotes the interaction with the external magnetic field. In the case of the hyperfine structure splitting this field is generated by the nucleus. In $g$-factor experiments a homogenoeus external field is applied.

models. The Bohr–Weisskopf effect for a hydrogenlike ion can be obtained from a measurement by

$$\epsilon^{(1s)} = \frac{\Delta E^{(1s)}_{\mathrm{Dirac}} + \Delta E^{(1s)}_{\mathrm{QED}} - \Delta E^{(1s)}_{\mathrm{Exp}}}{\Delta E^{(1s)}_{\mathrm{Dirac}}}, \tag{10}$$

where $\Delta E^{(1s)}_{\mathrm{Dirac}}$ is the value of the $1s_{1/2}$-hyperfine structure splitting including the nuclear charge distribution, $\Delta E^{(1s)}_{\mathrm{QED}}$ is the QED correction to the hyperfine structure splitting for the $1s_{1/2}$ state, and $\Delta E^{(1s)}_{\mathrm{Exp}}$ is the experimental value of the $1s_{1/2}$ hyperfine structure splitting. The first and the last of these quantities are well known, and the QED value is also known but put under test when a similar experiment is carried out on the $2s_{1/2}$ state of a lithiumlike ion, where a similar formula has to be applied. The expected ratio for the Bohr–Weisskopf effect is $\epsilon^{(2s)}/\epsilon^{(1s)} = 1.078$ for the case of $^{209}$Bi [106]. This quantity has to be tested by experiments. The QED contributions have to be known very precisely, and in addition to the diagrams shown in Figure 8, those corresponding to electron–electron interactions have to be taken into account at least to order $\alpha^2$. A few of them are displayed in Figure 9. Their value was estimated by Shabaev and co-workers [90, 105, 106, 108]. The above proposal was taken up already. A precision search was started at GSI. However, it did not yet yield any positive result [110] although the region under consideration was investigated very carefully. Due to technical problems, the search is not yet completed and therefore any high-precision test of the QED contributions to the hyperfine structure splitting in heavy highly charged ions is still not performed. For $^{209}$Bi, theoretical and experimental values are displayed in Table II.

In addition to the hyperfine structure splitting, the Feynman diagrams of Figure 8 also represent the QED corrections of order $\alpha$ to the $g$ factor of bound electrons. Whereas the magnetic field is generated by the spinning nucleus for the hyperfine structure splitting case, it is externally applied for $g$-factor measurements

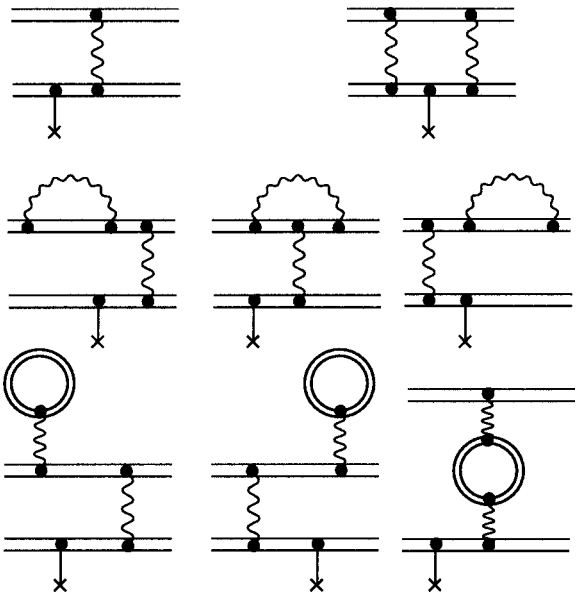

*Figure 9.* A few diagrams for interelectronic-interaction QED corrections to lithium-like ions.

*Table II.* Recent detailed theoretical predictions for the hyperfine structure splitting of the ground state in hydrogenlike and lithiumlike bismuth. For $^{209}Bi^{82+}$, the QED corrections and the relativistic one-electron value (including the finite nuclear-size effect) were taken from [104]. The separate finite nuclear-size effect was obtained by subtracting the corresponding value of a point-like nucleus calculated by Formula (8) (without $\delta$, $\epsilon$, and $\chi_{\mathrm{QED}}$). The Bohr–Weisskopf effect is given in [105]. For $^{209}Bi^{80+}$, all values were taken from [105]

| | $^{209}Bi^{82+}$ | $^{209}Bi^{80+}$ |
|---|---|---|
| Relativistic one-electron value | 5.8393(3) | 0.95849 |
| Finite nuclear-size effect | −0.6482(7) | −0.1138(2) |
| Bohr–Weisskopf effect | −0.061(27) | −0.0134(2) |
| One-electron QED (order $\alpha$) | −0.0298 | −0.0051(2) |
| Interelectronic interaction | | |
| of first order in $1/Z$ | | −0.02948 |
| of second and higher orders in $1/Z$ | | 0.00024(12) |
| estimate for QED correction [eV] | | 0.00018(9) |
| Theory, total [eV] | 5.100(27) | 0.7971(2) |
| Experiment [eV] | 5.0840(8) [80] | 0.820(26) [109] |
| | 5.0843(4) [82] | |

where the Zeeman effect is investigated. These experiments therefore employ much weaker but homogeneous magnetic fields of only several T which, on the other hand, are much better known and therefore allow much more precise theoretical predictions. The magnetic moment of a charge $q$ of mass $m_q$ is connected with its angular momentum $\mathbf{J}$ by

$$\boldsymbol{\mu} = g_j \frac{q}{2m_q} \mathbf{J}, \tag{11}$$

where $g_j$ is the $g$ factor of this particular charge. For an electron, the constant in Equation (11) is expressed as the Bohr magneton $\mu_\mathrm{B} = (e\hbar)/(2m_\mathrm{e}) \approx 0.579 \times 10^{-4}$ eV/T. The magnetic moment of an electron is

$$\boldsymbol{\mu}_\mathbf{J} = -g_j \mu_\mathrm{B} \frac{\mathbf{J}}{\hbar}, \tag{12}$$

where $\mathbf{J}$ denotes now the total angular momentum of the electron. For a free electron, the total angular momentum is equal to its spin $\mathbf{S}$, and the Dirac theory yields $g_\mathrm{free} = 2$. The deviations from this value due to QED were already given in the introduction. For bound electrons, a number of additional corrections appear. The most important is the transition from $S$ to $J$, because only the total angular momentum operator commutes with the Hamiltonian for a bound electron. This modification of the $g$ factor is sometimes called 'relativistic correction' and sometimes 'due to spin-orbit coupling'. However, it is not a 'correction' at all but is entirely contained in the Dirac equation. The $g$ factor of a bound electron due to this was already obtained by Breit in 1928 [111] (cf. also [112] and [113] for a detailed derivation). It is given by

$$g_{j,1s_{1/2}} = \frac{2}{3}\left(1 + 2\sqrt{1-(Z\alpha)^2}\right), \tag{13}$$

$$g_{j,2s_{1/2}} = \frac{2}{3}\left(1 + 2\sqrt{\frac{1+\sqrt{1-(Z\alpha)^2}}{2}}\right) \tag{14}$$

for the $1s_{1/2}$ and $2s_{1/2}$ states in hydrogenlike ions. This value again is modified due to quantum electrodynamical effects and also due to nuclear properties. Equations (13) and (14) were obtained employing wave functions for a point-like nuclear charge distribution. Extended nuclei lead to the finite-size correction which amounts to up to $10^{-3}$ for uranium. This correction is easy to handle and limits are put by the insufficiently known nuclear charge distribution which leads to an uncertainty of the order $10^{-7}$ for uranium but much less for medium-range and low $Z$. The finite nuclear mass leads to a recoil correction similar to the Lamb shift. However, for the $g$ factor no complete correction to all orders in $Z\alpha$ is known yet, and the existing values from a perturbation series in $Z\alpha$ [114, 115] are justified only for small $Z$ with an uncertainty of at least 1% in the region of carbon [116].

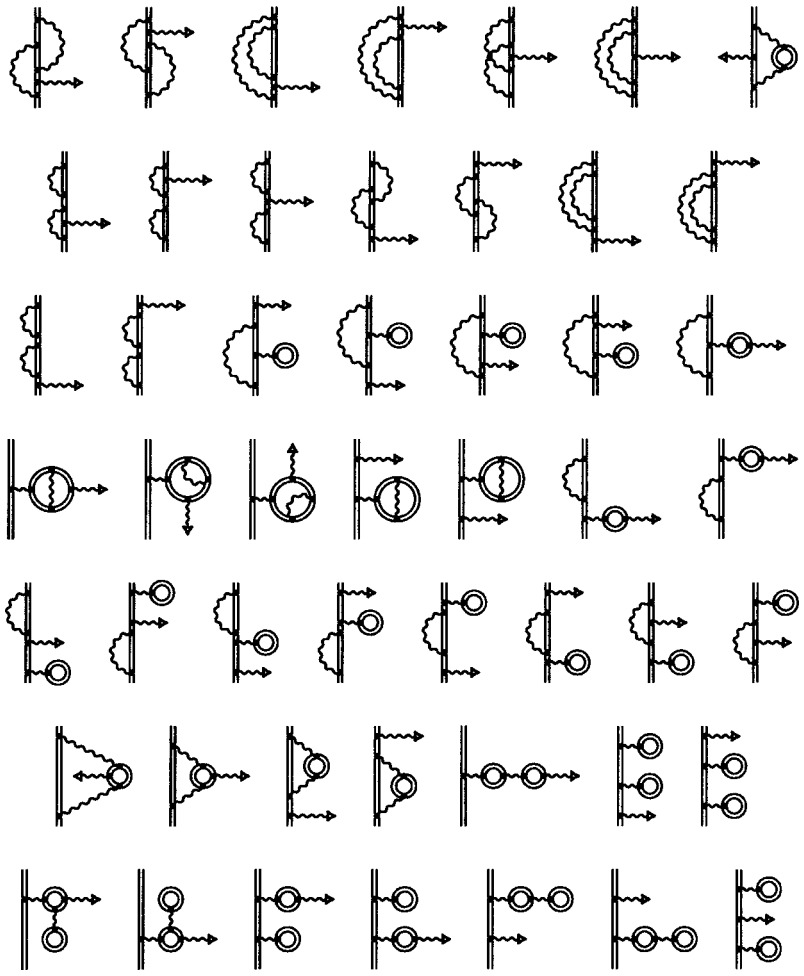

*Figure 10.* Graphs of order $(\alpha/\pi)^2$ to the $g$ factor of a bound electron and to the hyperfine structure in hydrogenlike atoms. The interaction with the magnetic field is denoted by a triangle. The figure is taken from [118].

All contributions resulting from the quantum electrodynamical corrections of order $(\alpha/\pi)$ (Figure 8) were first calculated by Persson *et al.* [117] and with slightly increased precision by Beier *et al.* [118]. For historical reasons, for the $g$ factor the expansion in $\alpha$ is referred to as expansion in $(\alpha/\pi)$, and we keep this terminology. Diagrams of order $(\alpha/\pi)^2$ (given in Figure 10) or higher have not yet been considered non-perturbatively in $Z\alpha$. Recently, investigations on a $Z\alpha$ expansion have been carried out [119] which indicate that the leading term in such a series for *each* order in $(\alpha/\pi)$ is given by

$$\Delta g_{\alpha^n} = 2A^{(2n)}\left(\frac{\alpha}{\pi}\right)^n \frac{1}{6}(Z\alpha)^2, \tag{15}$$

*Table III.* Known theoretical contributions to the $g$ factor of an electron bound in the ground state of $^{12}C^{5+}$. All values are given in units of $10^{-9}$. The uncertainty for the recoil results from the $Z\alpha$ expansion that is employed [116]. The values for the QED of order $(\alpha/\pi)$ are taken from [118]. The uncertainty for the order-$(\alpha/\pi)^2$ value is estimated to be 100% (cf. the discussion in the text). The error margins for the 'total' value are due to the $(Z\alpha)$ expansion for the recoil contribution, the numerical uncertainties for the QED effects of order $(\alpha/\pi)$, and the estimated uncertainty for the bound-state QED contribution of order $(\alpha/\pi)^2$

| Contribution to $g$ | Numerical value (in $10^{-9}$) |
|---|---|
| from Dirac eq. | 1998721354.2 |
| fin. nuc. size | 0.4 |
| recoil | 87.5(9) |
| total QED, order $(\alpha/\pi)$: | 2323663.9(12) |
| free QED, $(\alpha/\pi)^2$ to $(\alpha/\pi)^4$ | −3515.1 |
| bound QED, $(\alpha/\pi)^2\,(Z\alpha)^2$ | −1.1(11) |
| total: | 2001041589.8(9)(12)(11) |

where $A^{(2n)}$ is the corresponding term in the expansion in powers of $(\alpha/\pi)$ for $g/2$ of the *free* electron (cf. [2]). $A_1^{(4)} = 197/144 + (1/2 - 3\ln 2)\zeta(2) + 3/4\zeta(3) = -0.328\,478\,965\ldots$, where $\zeta(n)$ is Riemann's $\zeta$ function [120]. Investigations for the hyperfine structure splitting have shown, however, that the $Z\alpha$ expansion is not feasible at all to approximate radiative corrections for even medium-range $Z$ [101] and any result of such an approximation should therefore be considered with enormous care. In Table III we present all known theoretical contributions to the $g$ factor of hydrogenlike $^{12}C$. The bound-state QED contribution of order $(\alpha/\pi)$ can be obtained by subtracting this contribution for the free electron from the total value for that order. This gives $8443(12)\times 10^{-10}$ which has to be compared with $7422 \times 10^{-10}$ from the the corresponding $Z\alpha$ expansion [121]. It is clear that the available terms of the $Z\alpha$ expansion considerably underestimate the value even for the low $Z = 6$. For hydrogenlike carbon, an experiment was carried out which yielded a precision similar to the theoretical one [122, 123]. At this level, it becomes possible even to evaluate a new high-precision value for the electron mass that is given elsewhere in this volume [124].

Direct measurements of $g$ factors in elements heavier than carbon have not been carried out up to now. They are under way for oxygen and the results are rather promising [125]. However, if the lifetime of the higher of the two hyperfine-structure splitting levels is measured it is also possible to derive a value for the $g$ factor of the electron. This was pointed out by Shabaev [126]. The transition proba-

bility $w$ between ground-state hyperfine-structure sublevels in a hydrogen-like ion, including QED and nuclear corrections, is given by

$$w = \frac{\alpha}{3}\frac{(\Delta E)^3}{m^2}\frac{I}{2I+1}\left[g^{(\mathrm{e})} - g_I^{(\mathrm{n})}\frac{m}{m_\mathrm{p}}\right]^2. \tag{16}$$

Here $\Delta E$ is the transition energy, $g^{(\mathrm{e})}$ is the bound-electron $g$ factor defined above and $g_I^{(\mathrm{n})}$ is the nuclear $g$ factor. For the lowest-order QED and for a pointlike nucleus a connetion between $w$ and $g^{(\mathrm{e})}$ has been derived first in [127].

The lifetime of the upper hyperfine structure level in $^{209}\mathrm{Bi}^{82+}$ was measured to be $\tau_{\mathrm{exp}} = 397.5(1.5)\ \mu$s by Winter *et al.* [82]. Using Equation (16) and employing the experimental value of the hyperfine splitting $\Delta E$ together with the transition amplitude for $^{209}\mathrm{Bi}^{82+}$, the experimental value of the bound-electron $g$ factor is found to be 1.7343(33). This result is in remarkable good agreement with the theoretical value of 1.7310 for $^{209}\mathrm{Bi}^{82+}$. Also the value for $^{207}\mathrm{Pb}^{81+}$, measured by Seelig *et al.* [81], was found to be in good agreement with the theoretical prediction. Only the older measurement of Klaft *et al.* [80] yielded a shorter lifetime than predicted by theory. This triggered many investigations in the past. Only recently, the puzzle was solved by reinvestigating that experiment [110].

The high precision in $g$-factor measurements could also be used to reinvestigate the nuclear magnetic properties, in particular the nuclear magnetic moments themselves that enter the above formulae (8) and (16) via $\mu$ and $g_I$, respectively. It was pointed out [128] that due to the necessary corrections used in the old experiments, they might be less precisely known than stated or the tabulated values are simply wrong. We therefore conclude this section by pointing to the urgent need of reinvestigation also for the nuclear magnetic moments which became obvious by very precise experiments and calculations of QED effects.

## 4. Electroweak radiative corrections

Parity-nonconserving (PNC) neutral-current effects, as predicted by the standard electroweak gauge theory, have been observed in a wide variety of processes in atomic physics. Studying PNC in atomic systems provides an interesting possibility to deduce informations on the standard model of electroweak interactions independent of high-energy physics experiments. In principle, the weak interaction also contains parity-conserving terms, but it is much more difficult to observe these terms in experiments due to the smallness of these contributions compared to the also parity-conserving electromagnetic interactions. Therefore, parity-violation effects, both theoretically and experimentally, are investigated very intensively in today's atomic physics. The PNC originates from the weak interaction of atomic electrons with the nucleus and with the vacuum fluctuations of the electroweak gauge boson fields [129, 130]. Comparing experimental results with the theoretical predictions of the standard model again allows a glance on possible new physics

beyond the standard model, due to the high precision which is possible for theoretical calculations in atomic physics. Possible discoveries might be, e.g., a second $Z$ boson or supersymmetric counterparts of existing particles.

The most precise recent experiment was carried out by measuring the $7s_{1/2} \rightarrow 6s_{1/2}$ transition probability in atomic (i.e., neutral) $^{133}_{55}$Cs where the weak charge $Q_{\mathrm{W}}$ of the nucleus is probed. To lowest order ('tree-level'), $Q_{\mathrm{W}}$ is given by

$$Q_{\mathrm{W}} = Z\left(1 - 4\sin^2\Theta_{\mathrm{W}}\right) - N, \tag{17}$$

where $\sin^2\Theta_{\mathrm{W}}$ is the weak mixing angle ('Weinberg angle', $\sin^2\Theta_{\mathrm{W}} = 0.2224(19)$ [66]) and $N$ is the number of the neutrons in the nucleus under consideration. Adding radiative corrections, one obtains within the standard model $Q_{\mathrm{W}} = -73.20(13)$ for this system [131]. The experimental value was found to be $Q_{\mathrm{W}} = -72.06(28)_{\mathrm{exp.}}(34)_{\mathrm{theo.}}$ [132] which differs slightly from the standard-model value. This measurement is thought to be the first indication of the long-looked-for 'anapole moment' of the atomic nucleus [133] which is a parity-violation effect within the nucleus due to the weak interaction and manifests itself by a toroidal dipole moment. It was first proposed by Zel'dovitch just after the discovery of parity violation [134]. A detailed recent discussion can be found in [135] which also contains all important references on the subject. The discrepancy between $Q_{\mathrm{W\,standard\,model}}$ and $Q_{\mathrm{W\,Cs}\,7s\rightarrow 6s}$, however, may be simply due to the underestimation of theoretical uncertainties in the calculations for the Cs system [136] and does not yet clearly prove new physics beyond the standard model. Here, we face the general problem of atomic many-electron systems that although very precise calculations are possible in principle, they are difficult to handle due to the enormous amount of computer power that is required for these tasks.

In highly charged ions, on the other hand, the binding to the nucleus dominates by far the electron–electron interaction which may be considered as a perturbation. The spin-independent part of an effective Hamiltonian for a zero-momentum transfer interaction between a bound electron and a nucleus, mediated by a $Z_0$ boson, is given by

$$\hat{H}_{\mathrm{W}}(\mathbf{r}) = -\frac{G_{\mathrm{F}}}{2\sqrt{2}} Q_{\mathrm{W}}\, \rho_{\mathrm{N}}(\mathbf{r})\gamma_5, \tag{18}$$

where $G_{\mathrm{F}}$ denotes the Fermi constant, $\rho_{\mathrm{N}}(r)$ is the nuclear density and $\gamma_5$ is the Dirac matrix. Due to the parity-violating exchange of $Z$ bosons, every electron state has a small admixture of a wave function with opposite parity, $\Psi \rightarrow \Psi + \mathrm{i}\eta\Psi'$, where the coefficient $\mathrm{i}\eta$ is pure imaginary because of the $T$-invariance of the Hamiltonian (18). Accordingly, the amplitudes of the different processes in atoms look as follows [130]:

$$A = A_0 + \mathrm{i}\eta A_1, \tag{19}$$

where $A_0$ is the amplitude of the basic process and $A_1$ is the amplitude of the process caused by parity violation. The 'degree of the parity violation' $P$ in an

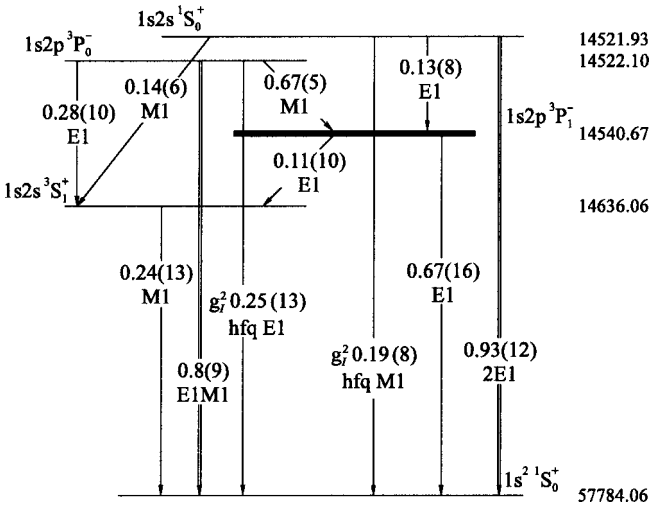


*Figure 11.* Energy-level scheme of the first excited states of heliumlike gadolinium. Numbers on the right-hand side indicate the ionization energies in eV. The partial probabilities of radiative transitions are given in $s^{-1}$. Numbers in parentheses indicate powers of 10. The large radiative width for the $1s2p^3P_1$ state is indicated as a bold line. The double lines denote two-photon transitions.

atomic process can be defined as [130]

$$P = 2\eta\frac{A_1}{A_0} = 2\eta\left(\frac{W_1}{W_0}\right)^{1/2}, \tag{20}$$

where $W_0$, $W_1$ are the probabilities corresponding to the amplitudes $A_0$ and $A_1$, respectively.

Electroweak radiative corrections were considered both for neutral atoms, e.g., in [137] and in the newer literature dealing with the situation in Cs ([136] and references therein) and also for highly charged hydrogen-like ions [138, 139]. The consideration of these radiative corrections becomes necessary because they can contribute up to 10% to the magnitude of PNC effects.

For experiments, a promising situation occurs in heavy heliumlike ions due to the near-degeneracy of two levels with opposite parities, $2^1S_0$ and $2^3P_0$. These levels cross near the nuclear charge numbers $Z = 64$ (gadolinium) as well as close to $Z = 92$ (uranium). The case of uranium was elsewhere considered in detail [140]. Here we restrict our consideration the heliumlike highly charged ions of gadolinium ($Z = 64$) and europium ($Z = 63$). Especially we consider a quenching-type experiment with interference of hyperfine- and weak-quenched transitions [141]. Such an experiment would require the use of a polarized highly-charged ion beam together with a beam-foil time-of-flight technique, a rather challenging task for experimentalists.

The standard parity violation situation in atoms concerns the $M1$ transition with an admixture of the $E1$ transition. For heliumlike gadolinium and europium, the

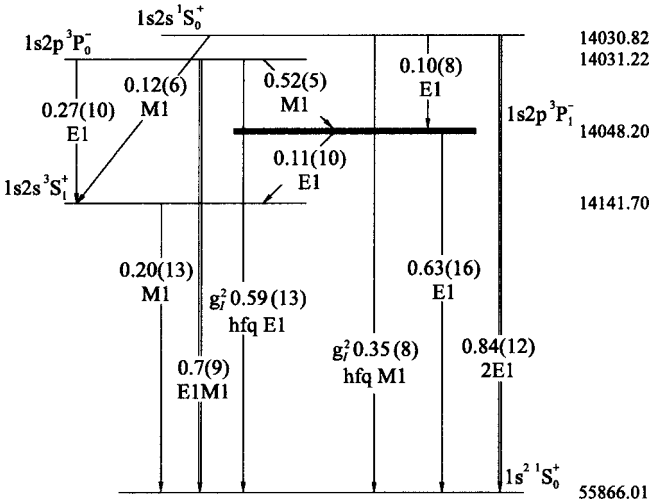


*Figure 12.* Energy-level scheme of the first excited states of heliumlike europium. Notations are the same as in Figure 11.

energy level scheme is shown in Figures 11 and 12, respectively. The one-photon hyperfine-quenched transition $2^1S_0 \to 1^1S_0$, via the magnetic photon emission ($M1$), is due to the hyperfine mixing of the $2^1S_0$ and $2^3S_1$ levels. The weak interaction of electrons with the nucleus also opens another one-photon decay channel $2^1S_0 \to 1^1S_0$, via the electric photon ($E1$) emission through the mixing of the $2^1S_0$ and $2^3P_1$ levels by the operator $H_{\rm W}$ in Equation (18). As a result, the total amplitude $A$ in Equation (19) is represented by the mixture of the basic $M1$ (magnetic photon) amplitude $A_0 \equiv A_s$ and the additional $E1$ (electric photon) amplitude $A_1 \equiv A_p$. The corresponding transitions rates are $W_s$ and $W_p$, respectively. The weak mixing coefficient $\eta$ in Equation (19) is determined by

$$\mathrm{i}\eta\Delta_0 = \langle 2^3P_0 | \hat{H}_{\rm W} | 2^1S_0 \rangle, \tag{21}$$

where $\Delta_0 = E_{2^1S_0} - E_{2^3P_0}$. The theoretical predictions for europium and gadolinium are listed in Table IV. Due to the admixture of states of opposite parity, in a polarized-beam experiment a small asymmetry in the number of emitted photons per direction should become visible, expressed by

$$\mathrm{d}W(\boldsymbol{n}) = \frac{W_s}{4\pi}\big[1 + \varepsilon(\zeta \cdot \boldsymbol{n})\big]\mathrm{d}\Omega, \tag{22}$$

where $\boldsymbol{n}$ indicates the direction of the photon emission and $\zeta$ is the unit vector in direction of the polarization of the ion. The coefficient of asymmetry is given by $\varepsilon = 3\lambda_0\eta R/(I+1)$ with $R = \sqrt{W_p/W_s}$. Here $\lambda_0 \leqslant 1$ is the degree of polarization.

In gadolinium, $\mathrm{i}\eta\Delta_0 = \mathrm{i}0.155 \times 10^{-6}$ eV. The total asymmetry effect turns out to be $2\varepsilon \simeq 0.78\lambda_0 \times 10^{-3}$, what is unusually large for parity-violation experiments. However, unfortunately the lifetime of the $2^1S_0$ level defined by the $2E1$

*Table IV.* The theoretical results for transition rates $W_s$, $W_p$ and for the weak mixing factor for heliumlike europium and gadolinium

| Nucl. | $W_s$ ($s^{-1}$) | $W_p$ ($s^{-1}$) | $\eta$ |
|---|---|---|---|
| $^{151}_{63}$Eu | $0.68 \times 10^{8}$ | $0.11 \times 10^{14}$ | $0.33 \times 10^{-6}$ |
| $^{155}_{64}$Gd | $0.58 \times 10^{6}$ | $0.75 \times 10^{11}$ | $0.91 \times 10^{-6}$ |

two-photon transition is about one order of magnitude smaller than the hyperfine-quenched $2^3P_0$ lifetime. This implies a strong background in experiments with $Gd^{62+}$ ions.

In europium the weak asymmetry effect reduces up to $2\varepsilon \simeq 0.23\lambda_0 \times 10^{-3}$. However, the $2^1S_0$ level lives significantly longer then the hyperfine-quenched $2^3P_0$ level. The $2^1S_0$ lifetime equals to about 1.19 ps and corresponds to a decay length of about 0.1 mm in the laboratory. The peculiarity of the situation is that unlike in standard hyperfine-quenching experiments we are not aiming at the measurement of the lifetime defined in our case by the two-photon transition. The experiment should result in a measurement of the ratio $\Delta n/n_0$, where $n_0 \pm \Delta n/2$ are the numbers of counts for two directions $\zeta$ of the beam polarization. This ratio is directly proportional to the weak interaction matrix element: $\Delta n/n_0 = 2\varepsilon$.

Since photons being observed in this experiment originate from the single-photon decays of the hyperfine- and weak-mixed $F = I$ state, the success of the experiment will depend on the production of a significant degree of polarization for this state of the heliumlike ion. This is a task to address to the experimentalists in order to employ the advantages of heavy highly charged ions for parity-violation investigations and the search for possible new physics beyond the standard model.

## 5. Summary

During the last two decades there has been increasing interest in quantum electrodynamics of strong fields and parity-violating effects in atoms. For one-electron systems, the fundamental QED contributions can be tested most directly in strong fields. Therefore, in this review we considered the present status of the Lamb-shift predictions for hydrogenlike uranium and lead. We emphasized the necessity to include even the second-order QED corrections in the Lamb-shift calculations. The recent evaluation of the two-photon self-energy contribution reduces the main uncertainty in the theoretical Lamb-shift predictions. For hydrogen, the current experimental and theoretical precision not only allows high-precision tests of QED but also to determine fundamental constants like $R_\infty$ with high accuracy. Quantum electrodynamics might therefore be helpful even for looking for new physics beyond the standard model such as a variation of the fundamental constants.

We demonstrate that hyperfine splitting effects are also suitable for tests of QED in strong electromagnetic fields. For any test of QED in strong magnetic fields by hyperfine-structure splitting, the Bohr–Weisskopf effect is the main source of uncertainty in the present predictions, together with possibly erroneously known magnetic moments of the nuclei. In contrast, experiments on the $g$ factor yield an up-to-now unmatched precision and agreement with theory on the same level for any bound state system heavier than hydrogen.

Finally we discussed parity violation effects in few-electron systems. Up to now, experimental data of atomic parity violation effects are available only for neutral atoms. For highly charged ions with a $Z$ close to $Z = 64$, however, the effect of PNC is ten times larger as in neutral atoms because of the near-degeneracy of two levels for $Z = 64$. In particular, to measure the parity-violation effect for heliumlike gadolinium ($Z = 64$) and europium ($Z = 63$), we propose a quenching-type experiment with interference of hyperfine- and weak-quenched transitions.

## Acknowledgements

T. B. and S. Z. would like to thank Prof. V. M. Shabaev and V. A. Yerokhin for many valuable discussions. We are also grateful to G. Werth and his team for providing us with amazing experimental results prior to publication. U. D. J. would like to acknowledge support from the Deutscher Akademischer Austauschdienst (DAAD), and he would like to thank the Laboratoire Kastler–Brossel for kind hospitality. G. S., G. P., and S. Z. acknowledge financial support from BMBF, DFG, and GSI. I. A. G., L. N. L., and A. V. N. are grateful to the Technische Universität Dresden and the Max-Planck-Institut für Physik komplexer Systeme (MPI) for the hospitality and for financial support from the MPI, DFG, and RFBR (grant no. 99-02-18526).

## References

1. Van Dyck, Jr., R. S., Schwinberg, P. B. and Dehmelt, H. G., *Phys. Rev. Lett.* **59** (1987), 26.
2. Hughes, V. W. and Kinoshita, T., *Rev. Mod. Phys.* **71** (1999), 133.
3. Jeffrey, A.-M., Elmquist, R. E., Lee, L. H. and Dziuba, R. F., *IEEE Trans. Inst. Meas.* **46** (1997), 264.
4. Pachucki, K., *Phys. Rev. A* **60** (1999), 3593.
5. Karshenboim, S. G., *Can. J. Phys.* **77** (1999), 241.
6. Pieper, W. and Greiner, W., *Z. Phys.* **218** (1969), 327.
7. Zel'dovich, Y. B. and Popov, V. S., *Usp. Fiz. Nauk* **105** (1971), 403 [*Sov. Phys. – Usp.* **14** (1972), 673–694].
8. Müller-Nehler, U. and Soff, G., *Physics Reports* **246** (1994), 101.
9. Ionescu, D. C., Reinhardt, J., Müller, B. and Greiner, W., *Phys. Rev. A* **38** (1988), 616.
10. Beyer, H. F., Menzel, G., Liesen, D., Gallus, A., Bosch, F., Deslattes, R., Indelicato, P., Stöhlker, T., Klepper, O., Moshammer, R., Nolden, F., Eickhoff, H., Franzke, B. and Steck, M., *Z. Phys. D* **35** (1995), 169.

11. Beyer, H. F. and Stöhlker, T., Test of QED in high-Z hydrogen-like systems, In: E. Zavattini, D. Bakalov and C. Rizzo (eds), *Frontier Tests of QED and Physics of the Vacuum*, Heron Press, Sofia, 1998, pp. 356–370.
12. Stöhlker, T., Mokler, P. H., Bosch, F., Dunford, R. W., Franzke, F., Klepper, O., Kozhuharov, C., Ludziejewski, T., Nolden, F., Reich, H., Rymuza, P., Stachura, Z., Steck, M., Swiat, P. and Warczak, A., *Phys. Rev. Lett.* **85** (2000), 3109.
13. Beyer, H. F., Liesen, D., Bosch, F., Finlayson, K. D., Jung, M., Klepper, O., Moshammer, R., Beckert, K., Eickhoff, H., Franzke, B., Nolden, F., Spädtke, P. and Steck, M., *Phys. Lett. A* **184** (1994), 435.
14. Mokler, P. H., Stöhlker, T., Kozhuharov, C., Moshammer, R., Rymuza, P., Stachura, Z. and Warczak, A., *J. Phys. B* **28** (1995), 617.
15. Stöhlker, T., Mokler, P. H., Geissel, H., Moshammer, R., Rymuza, P., Bernstein, E. M., Cocke, C. L., Kozhuharov, C., Münzenberg, G., Nickel, F., Scheidenberger, C., Stachura, Z., Ullrich, J. and Warczak, A., *Phys. Lett. A* **168** (1992), 285.
16. Franosch, T. and Soff, G., *Z. Phys. D* **18** (1991), 219.
17. Brown, G. E., Langer, J. S. and Schaefer, G. W., *Proc. R. Soc. London A* **251** (1959), 92.
18. Desiderio, A. M. and Johnson, W. R., *Phys. Rev. A* **3** (1971), 1267.
19. Mohr, P. J., *Ann. Phys. (New York)* **88** (1974), 26.
20. Mohr, P. J., *Phys. Rev. Lett.* **34** (1975), 1050.
21. Snyderman, N. J., *Ann. Phys. (New York)* **211** (1991), 43.
22. Blundell, S. A. and Snyderman, N. J., *Phys. Rev. A* **44** (1991), R1427.
23. Uehling, E. A., *Phys. Rev.* **48** (1935), 55.
24. Wayne Fullerton, L. and Rinker, Jr., G. A., *Phys. Rev. A* **13** (1976), 1283.
25. Borie, E. and Rinker, G. A., *Rev. Mod. Phys.* **54** (1982), 67.
26. Hylton, D. J., *Phys. Rev. A* **32** (1985), 1303.
27. Wichmann, E. H. and Kroll, N. M., *Phys. Rev. A* **101** (1956), 843.
28. Gyulassy, M., *Nucl. Phys. A* **244** (1975), 497.
29. Soff, G. and Mohr, P., *Phys. Rev. A* **38** (1988), 5066.
30. Fainshtein, A. G., Manakov, N. L. and Nekipelov, A. A., *J. Phys. B* **24** (1991), 559 (Misprints of volume number and year in the header of the printed paper!)
31. Persson, H., Lindgren, I., Salomonson, S. and Sunnergren, P., *Phys. Rev. A* **48** (1993), 2772.
32. Mohr, P. J. and Soff, G., *Phys. Rev. Lett.* **70** (1993), 158.
33. Beier, T., Mohr, P. J., Persson, H. and Soff, G., *Phys. Rev. A* **58** (1998), 954.
34. Goidenko, I. A., Labzowsky, L. N., Nefiodov, A. V., Plunien, G., Soff, G., Zschocke, S., Second-order self energy calculations for tightly bound electrons in hydrogenlike ions, In: S. G. Karshenboim and F. S. Pavone (eds), *Hydrogen Atom II*, *Proceedings of the Satellite Meeting "Precision Physics of Simple Atomic Systems" of the 17. ICAP Conference*, Springer, in press.
35. Mitrushenkov, A., Labzowsky, L., Lindgren, I., Persson, H. and Salomonson, S., *Phys. Lett. A* **200** (1995), 51.
36. Mallampalli, S. and Sapirstein, J., *Phys. Rev. Lett.* **80** (1998), 5297.
37. Goidenko, I., Labzowsky, L., Nefioodv, A., Plunien, G. and Soff, G., *Phys. Rev. Lett.* **83** (1999), 2312.
38. Karshenboim, S. G., *Zh. Eksp. Teor. Fiz.* (1993).
39. Yerokhin, V. A., *Phys. Rev. A* **62** (2000), 012508.
40. Manohar, A. V. and Stewart, I. W., *Phys. Rev. Lett.* **85** (2000), 2248.
41. Pachucki, K., *Ann. Phys. (New York)* **226** (1993), 1.
42. Beier, T. and Soff, G., *Z. Phys. D* **8** (1988), 129.
43. Schneider, S. M., Greiner, W. and Soff, G., *J. Phys. B* **26** (1993), L529.
44. Plunien, G., Beier, T., Soff, G. and Persson, H., *EPJD* **1** (1998), 177.
45. Beier, T., Plunien, G., Greiner, M. and Soff, G., *J. Phys. B* **30** (1997), 2761.

46. Lindgren, I., Persson, H., Salomonson, S., Karasiev, V., Labzowsky, L., Mitrushenkov, A. and Tokman, M., *J. Phys. B* **26** (1993), L503.
47. Persson, H., Lindgren, I., Labzowsky, L. N., Plunien, G., Beier, T. and Soff, G., *Phys. Rev. A* **54** (1996), 2805.
48. Mallampalli, S. and Sapirstein, J., *Phys. Rev. A* **54** (1996), 2714.
49. Mohr, P. J., Plunien, G. and Soff, G., *Physics Reports* **293** (1998), 227.
50. Plunien, G., Müller, B., Greiner, W. and Soff, G., *Phys. Rev. A* **43** (1991), 5853.
51. Plunien, G. and Soff, G., *Phys. Rev. A* **51** (1995), 1119; ibid. **53** (1996), 4614(E).
52. Labzowsky, L. N., Nefiodov, A. V., Plunien, G., Beier, T. and Soff, G., *J. Phys. B* **29** (1996), 3841.
53. Artemyev, A. N., Shabaev, V. M. and Yerokhin, V. A. *Phys. Rev. A* **52** (1995), 1884.
54. Artemyev, A. N., Shabaev, V. M. and Yerokhin, V. A., *J. Phys. B* **28** (1995), 5201.
55. Shabaev, V. M., Artemyev, A. N., Beier, T., Plunien, G., Yerokhin, V. A. and Soff, G., *Phys. Rev. A* **57** (1998), 4235.
56. Sapirstein, J. R. and Yennie, D. R., Theory of hydrogenic bound states, In: T. Kinoshita (ed.), *Quantum Electrodynamics*, Advanced Series on Directions in High Energy Physics 7, World Scientific, Singapore, 1990, chapter 12, pp. 560–672.
57. Beier, T., Mohr, P. J., Persson, H., Plunien, G., Greiner, M. and Soff, G., *Phys. Lett. A* **236** (1997), 329.
58. Pachucki, K., Leibfried, D., Weitz, M. Huber, A., König, W. and Hänsch, T. W., *J. Phys. B* **29** (1996), 177.
59. Jentschura, U. D., Mohr, P. J. and Soff, G., *Phys. Rev. Lett.* **82** (1999), 53.
60. Jentschura, U. D., Mohr, P. J., Soff, G. and Weniger, E. J., *Comput. Phys. Commun.* **116** (1999), 28.
61. Jentschura, U. D. and Pachucki, K., *Phys. Rev. A* **54** (1996), 1853.
62. Jentschura, U. D., Soff, G. and Mohr, P. J., *Phys. Rev. A* **56** (1997), 1739.
63. Weniger, E.J., *Comput. Phys. Rep.* **10** (1989), 189.
64. Jentschura, U. D., Mohr, P. J., Soff, G., Calculation of QED effects in hydrogen, *Hyp. Interact.* (this issue).
65. Niering, M., Holzwarth, R., Reichert, J., Pokasov, P., Udem, Th., Weitz, M., Hänsch, T. W., Lemonde, P., Santarelli, G., Abgrall, M., Laurent, P., Salomon, C. and Clairon, A., *Phys. Rev. Lett.* **84** (2000), 5496.
66. Mohr, P. J. and Taylor, B. N., *Rev. Mod. Phys.* **72** (2000), 351.
67. Prestage, J. D., Tjoelker, R. L. and Maleki, L., *Phys. Rev. Lett.* **74** (1995), 3511.
68. Dzuba, V. A. and Flambaum, V. V., *Phys. Rev. A* **61** (2000), 034502.
69. Webb, J. K., Flambaum, V. V., Churchill, C. W., Drinkwater, M. J. and Barrow, J. D., *Phys. Rev. Lett.* **82** (1999), 884.
70. Dirac, P. A. M., *Nature (London)* **139** (1937), 323.
71. Marciano, W. J., *Phys. Rev. Lett.* **52** (1984), 489.
72. Barrow, J. D., *Phys. Rev. D* **35** (1987), 1805.
73. Damour, T. and Polyakov, A. M., *Nucl. Phys. B* **423** (1994), 532.
74. Carroll, S. M., *Phys. Rev. Lett.* **81** (1998), 3067.
75. Godone, A., Novero, C., Tavella, P. and Rahimullah, K., *Phys. Rev. Lett.* **71** (1993), 2364.
76. Bodwin, G. T. and Yennie, D. R., *Phys. Rev. D* **37** (1988), 498.
77. Hellwig, H., Vessot, R. F. C., Levine, M. W., Zitzewitz, P. W., Allan, D. W. and Glaze, D. J., *IEEE Trans. Inst. Meas.* **IM-19** (1970), 200.
78. Essen, L., Donaldson, R. W., Bangham, M. J. and Hope, E. G., *Nature (London)* **229** (1971), 110.
79. Zemach, A. C., *Phys. Rev.* **104** (1956), 1771.
80. Klaft, I., Borneis, S., Engel, T., Fricke, B., Grieser, R., Huber, G., Kühl, T., Marx, D., Neumann, R., Schröder, S., Seelig, P. and Völker, L., *Phys. Rev. Lett.* **73** (1994), 2425.

81. Seelig, P. Borneis, S., Dax, A., Engel, T., Faber, S., Gerlach, M., Holbrow, C., Huber, G., Kühl, T., Marx, D., Meier, K., Merz, P., Quint, W., Schmitt, F., Tomaselli, M., Völker, L., Winter, H., Würtz, M., Beckert, K., Franzke, B., Nolden, F., Reich, H., Steck, M. and Winkler, T., *Phys. Rev. Lett.* **81** (1998), 4824.
82. Winter, H., Borneis, S., Dax, A., Faber, S., Kühl, T., Marx, D., Schmitt, F., Seelig, P., Seelig, W., Shabaev, V. M., Tomaselli, M. and Würtz, M.: Bound electron $g$-factor in hydrogen-like bismuth, In: *GSI Scientific Report 1998*, GSI, DE-64291 Darmstadt, Germany, 1999, p. 87.
83. Crespo López-Urrutia, J. R., Beiersdorfer, P., Savin, D. W. and Widmann, K., *Phys. Rev. Lett.* **77** (1996), 826.
84. Crespo López-Urrutia, J. R., Beiersdorfer, P., Widmann, K., Birkett, B. B., Mårtensson-Pendrill, A.-M. and Gustavsson, M. G. H., *Phys. Rev. A* **57** (1998), 879.
85. Pyykkö, P., Pajanne, E. and Inokuti, M., *Int. J. Quantum Chem.* **7** (1973), 785.
86. Shabaev, V. M., Tomaselli, M., Kühl, T., Artemyev, A. N. and Yerokhin, V. A., *Phys. Rev. A* **56** (1997), 252.
87. Bohr, A. and Weisskopf, V. F., *Phys. Rev.* **77** (1950), 94.
88. Bohr, A., *Phys. Rev.* **81** (1951), 331.
89. Shabaev, V. M., *J. Phys. B* **27** (1994), 5825.
90. Shabaev, V. M., Shabaeva, M. B., Tupitsyn, I. I., Yerokhin, V. A., Artemyev, A. N., Kühl, T., Tomaselli, M. and Zherebtsov, O. M., *Phys. Rev. A* **57** 149 (1998); ibid. **58** (1998), 1610(E).
91. Labzowsky, L. N., Johnson, W. R., Soff, G. and Schneider, S. M., *Phys. Rev. A* **51** (1995), 4597.
92. Labzowsky, L., Nefiodov, A., Plunien, G., Soff, G. and Pyykkö, P., *Phys. Rev. A* **56** (1997), 4508.
93. Schneider, S. M., Schaffner, J., Greiner, W. and Soff, G., *J. Phys. B* **26** (1993), L581.
94. Finkbeiner, M., Fricke, B. and Kühl, T., *Phys. Lett. A* **176** (1993), 113.
95. Arima, A. and Horie, H., *Prog. Theor. Phys.* **11** (1955), 509.
96. Noya, H., Arima, A. and Horie, H., *Prog. Theor. Phys*. **8** (1958), 33.
97. Tomaselli, M., Schneider, S. M., Kankeleit, E. and Kühl, T., *Phys. Rev. C* **51** (1995), 2989.
98. Tomaselli, M., Kühl, T., Seelig, P., Holbrow, C. and Kankeleit, E., *Phys. Rev. C* **58** (1998), 1524.
99. Beier, T., *Physics Reports* **339** (2000), 79.
100. Schneider, S. M., Greiner, W. and Soff, G., *Phys. Rev. A* **50** (1994), 118.
101. Persson, H., Schneider, S. M., Greiner, W., Soff, G. and Lindgren, I., *Phys. Rev. Lett.* **76** (1996), 1433.
102. Yerokhin, V. A., Shabaev, V. M. and Artemyev, A. N., *Pis'ma Zh. Eksp. Teor. Fiz.* **66** (1997), 19 [*JETP Lett.* **66**(1) (10 July 1997), 18–21]; E-print archive, physics/9905029 (1997) (http://xxx.lanl.gov).
103. Blundell, S. A., Cheng, K. T. and Sapirstein, J., *Phys. Rev. A* **55** (1997), 1857.
104. Sunnergren, P., Persson, H., Salomonson, S., Schneider, S. M., Lindgren, I. and Soff, G., *Phys. Rev. A* **58** (1998), 1055.
105. Shabaev, V. M., Artemyev, A. N., Zherebtsov, O. M., Yerokhin, V. A., Plunien, G. and Soff, G., *Hyp. Interact.* **127** (2000), 279.
106. Shabaev, V. M., Shabaeva, M. B., Tupitsyn, I. I. and Yerokhin, V. A., *Hyp. Interact*. **114** (1998), 129.
107. Shabaev, V. M., Hyperfine structure of highly charged ions, In: H. F. Beyer and V. P. Shevelko (eds), *Atomic Physics with Heavy Ions*, Springer, Berlin, Heidelberg, 1998, chapter VI, pp. 138–158.
108. Shabaeva, M. B. and Shabaev, V. M., *Phys. Rev. A* **52** (1995), 2811.
109. Beiersdorfer, P., Osterheld, A. L., Scofield, J. H., Crespo López-Urrutia, J. R. and Widmann, K., *Phys. Rev. Lett.* **80** (1998), 3022.

110. Borneis, S., Dax, A., Engel, T., Holbrow, C., Huber, G., Kühl, T., Marx, D., Merz, P., Quint, W., Schmitt, F., Seelig, P., Tomaselli, M., Winter, H., Beckert, K., Franzke, B., Nolden, F., Reich, H. and Steck, M., *Hyp. Interact.* **127** (2000), 305.
111. Breit, G., *Nature (London)* **122** (1928), 649.
112. Margenau, H., *Phys. Rev.* **57** (1940), 383.
113. Rose, M. E., *Relativistic Electron Theory*, Wiley, New York, 1961.
114. Faustov, R., *Phys. Lett.* **33B** (1970), 422.
115. Grotch, H., *Phys. Rev. A* **2** (1970), 1605.
116. Beier, T., Lindgren, I., Persson, H., Salomonson, S. and Sunnergren, P., *Hyp. Interact.* **127** (2000), 339.
117. Persson, H., Salomonson, S., Sunnergren, P. and Lindgren, I., *Phys. Rev. A* **56** (1997), R2499.
118. Beier, T., Lindgren, I., Persson, H., Salomonson, S., Sunnergren, P., Häffner, H. and Hermanspahn, N., *Phys. Rev. A* **62** (2000), 032510.
119. Eides, M. I. and Grotch, H., *Ann. Phys. (New York)* **260** (1997), 191.
120. Abramowitz, M. and Stegun, I. A., *Handbook of Mathematical Functions*, 8th edn, Dover, New York, 1972.
121. Grotch, H. and Hegstrom, R. A., *Phys. Rev. A* **4** (1971), 59.
122. Hermanspahn, N., Häffner, H., Kluge, H.-J., Quint, W., Stahl, S., Verdú, J. and Werth, G., *Phys. Rev. Lett.* **84** (2000), 427.
123. Häffner, H., Beier, T., Hermanspahn, N., Kluge, H.-J., Quint, W., Stahl, S., Verdú, J. and Werth, G., *Phys. Rev. Lett.* **85** (2000), 5308.
124. Werth, G., Häffner, H., Kluge, H.-J., Quint, W., Valenzuela, T. and Verdu, J., A possible new value for the electron mass from g-factor measurements on Hydrogen-like ions, this issue, 209.
125. Werth, G., private communication.
126. Shabaev, V. M., *Can. J. Phys.* **76** (1998), 907.
127. Schneider, S. M., Greiner, W. and Soff, G., *Z. Phys. D* **31** (1994), 143.
128. Gustavsson, M. G. H. and Mårtensson-Pendrill, A.-M., *Phys. Rev. A* **58** (1998), 3611.
129. Kriplovich, I., *Parity Nonconservation in Atomic Phenomena*, Gordon and Breach, New York, 1991.
130. Labzowsky, L., Klimchitskaya, G. and Dmitriev, Y. Y., *Relativistic Effects in the Spectra of Atomic Systems*, Institute of Physics Publishing, Bristol, 1993.
131. Marciano, W. J. and Rosner, J. L., *Phys. Rev. Lett.* **65** 2963 (1990); ibid. **68** (1992), 898(E).
132. Bennett, S. C. and Wieman, C. E., *Phys. Rev. Lett.* **82** 2484 (1999); ibid. **82** (1999), 4153(E); **83** (1999), 889(E).
133. Wood, C. S., Bennett, S. C., Cho, D., Masterson, B. P., Roberts, J. L., Tanner, C. E. and Wieman, C. E., *Science* **275** (1997), 1759.
134. Zel'dovich, Y. B., *Zh. Eksp. Teor. Fiz.* **33** (1957), 1531; [*JETP* **6** (1958), 1184].
135. Flambaum, V. V. and Murray, D. W., *Phys. Rev. C* **56** (1997), 1641.
136. Dzuba, V. A. and Flambaum, V. V., *Phys. Rev. A* **62** (2000), 052101.
137. Lynn, B. W. and Sandars, P. G. H., *J. Phys. B* **27** (1994), 1469.
138. Bednyakov, I., Labzowsky, L., Plunien, G., Soff, G. and Karasiev, V., *Phys. Rev. A* **61** (1999), 012103.
139. Bednyakov, I., Labzowsky, L., Soff, G., Plunien, G. and Karasiev, V., *Hyp. Interact.* **127** (2000), 301.
140. Schäfer, A., Soff, G., Indelicato, P., Müller, B. and Greiner, W., *Phys. Rev. A* **40** (1989), 7362.
141. Labzowsky, L. N., Nefiodov, A. V., Plunien, G., Soff, G., Marrus, R. and Liesen, D., *Phys. Rev. A* **63** (2001), 054501.